JOURNAL OF SCIENTIFIC AND TECHNOLOGICAL INNOVATIONS

Journal of Scientific and Technological Innovations 1: e205045
DOI: 10.3897/sti.e205045
https://sti.pensoft.net/

Review Article

Design, Functionalities, and Emerging Applications of $Ti_3C_2T_x$ MXene-Based Composites: A Review

Qui Thanh Hoai Ta[1], Nhiem Pham-Ngoc[2], Quynh Nhu Tran[3,4], Lu Thi Mong Thy[5], Jin-Seo Noh[6]

1 *Institute of Advanced Technology, Vietnam Academy of Science and Technology, Ho Chi Minh City, Vietnam*
2 *School of Chemical Engineering, University of Ulsan, Ulsan, Republic of Korea*
3 *Department of Condensed Matter Physics, Faculty of Science, Masaryk University, Brno, Czech Republic*
4 *Institute of Physics of Materials, Czech Academy of Sciences, Brno, Czech Republic*
5 *Ho Chi Minh City University of Industry and Trade, Ho Chi Minh City, Vietnam*
6 *Department of Physics and Semiconductor Science, Gachon University, Seongnam-si, Republic of Korea*

Corresponding author: Jin-Seo Noh (e-mail: jinseonoh@gachon.ac.kr)

Academic editor: Thanh-Binh Nguyen ♦ **Received:** 22 June 2026 ♦ **Accepted:** 11 August 2026 ♦ **Published:** 28 September 2026

Citation: Ta QTH, Pham NN, Tran QN, Lu TMT, Noh JS (2026) Design, Functionalities, and Emerging Applications of $Ti_3C_2T_x$ MXene-Based Composites: A Review. Journal of Scientific and Technological Innovations 1: e205045. doi: 10.3897/sti.e205045.

Abstract

The rise of two-dimensional (2D) materials is crucial for advancing modern life and industry. $Ti_3C_2T_x$ MXenes have attracted significant attention due to their conductivity, natural hydrophilicity, diverse termination groups, and impressive mechanical properties, offering unique advantages in practical applications. When $Ti_3C_2T_x$ MXene are combined with metal oxide semiconductors and polymers to create functional composites, their applications span multiple fields, including gas sensors, photocatalytic CO_2 reduction, and energy storage. This review will focus on the synthesis methods and physicochemical properties of $Ti_3C_2T_x$ MXene nanosheets, and will discuss their various applications. Finally, based on the pros and cons of the current research status, the challenges and opportunities for improving MXene-based composites are investigated. This review aims to summarize the latest research results in recent years, offering constructive insights for 2D materials studies.

Keywords

$Ti_3C_2T_x$ MXene, synthesis, properties, potential applications.

1. Introduction

It has been around 20 years since graphene oxide was first studied, sparking a surge in the development of two-dimensional (2D) materials such as metal-organic frameworks (MOFs), zeolitic imidazolate frameworks (ZIFs), and MXenes (Novoselov et al. 2004, Lehman et al. 2011, Stock and Biswas 2012, Ighalo et al. 2022, Thi et al. 2024). In 2011, MXenes joined the 2D materials class as the newest members. These MXenes can be prepared by etching polycrystalline nanolaminates of the MAX phase ($M_{n+1}AX_n$), where M signifies transition metals (e.g., Ti, Cr, Nb, Hf), A stands for group A elements (e.g., Si, Al), X is N/C, and n is an integer (1-4) (Ta et al. 2021, Tran et al. 2021b, Sreedhar et al. 2025). $Ti_3C_2T_x$ MXene is one of the first and most studied, which has become a benchmark for the entire MXene class. $Ti_3C_2T_x$ MXene, with abundant functional groups, exhibits unique properties such as high electrical conductivity (~25,000 $S \cdot cm^{-1}$), outstanding mechanical properties (Young's modulus of 330 GPa), electrochemical performance (volumetric capacitance of 1500 $F \cdot cm^{-3}$), and tunable hydrophilicity (Alhabeb et al. 2017, Anasori et al. 2017, Benchakar et al. 2020, Venkateshalu and Grace 2020, Ayodhya 2023).

Copyright by Qui Thanh Hoai Ta et al. This is an open access article distributed under the terms of the Creative Commons Attribution License (CC-BY 4.0), which permits unrestricted use, distribution, and reproduction in any medium, provided the original author and source are credited.

However, multilayered $Ti_3C_2T_x$ MXene also presents challenges in structural design and material modification due to its large block structure. These challenges can be mitigated by exfoliating it into monolayers or combining it with other materials. After hybridization or surface functionalization, MXene may experience a reduction in electrical conductivity, which can adversely affect its performance in certain applications. To address this limitation, constructing MXene-based heterostructures with highly conductive materials has emerged as an effective strategy to preserve efficient charge transport while enhancing the overall functional performance of the composite. In fact, an increasing number of scientists have focused on energy storage devices, which are applied in a wide range of applications, from renewable energy systems to electric vehicles and wearable electronics. Traditional batteries, however, have numerous disadvantages, such as low power density and limited lifespan. MXenes have been widely investigated as potential candidates for energy harvesting and storage in electronic devices, including supercapacitors, solar cells, and batteries, due to their multilayer structure and electrical conductivity (Shuck and Gogotsi 2020, Xu and Gogotsi 2020, Gogotsi and Huang 2021, Mohammadi et al. 2021, Naguib et al. 2021, Anasori and Gogotsi 2023, Barsoum and Gogotsi 2023, Gogotsi 2023, Sreedhar and Noh 2025b).

The progress has been made in the fields of gas sensors and photocatalytic oxidation. Moreover, both electrochemical reactions and photocatalytic oxidation reactions have been extensively studied, photocatalytic activity, primarily stimulated under illumination, presents more challenges than electrocatalytic reactions due to issues related to the separation of hole-electron pairs and charge transfer. Although several advancements have been achieved in this application, MXenes have been considered as metal sites for integration with traditional semiconductors such as ZnO, CdS, C_3N_4, and TiO_2 (Ta et al. 2022b, 2022a, 2024, Sreedhar et al. 2023a).

Although numerous review articles on $Ti_3C_2T_x$ MXenes have been published, most primarily concentrate on individual topics, including synthesis strategies, energy storage, photocatalysis, gas sensing, or CO_2 reduction (Sreedhar et al. 2022, 2023b, 2024, Sadashiva et al. 2024, Ajmal et al. 2025, Ghanbari et al. 2025, Mohtasim and Das 2025, Sreedhar and Noh 2025a). A review that systematically correlates synthesis methods, surface chemistry, interfacial engineering, and structure–property relationships with the performance of $Ti_3C_2T_x$-based composites in both photocatalysis, energy storage and sensing applications remains limited. Therefore, this review aims to provide an updated and integrated overview of recent advances in $Ti_3C_2T_x$ composites. Particular emphasis is placed on the influence of synthesis routes and surface functionalization on material properties, the underlying mechanisms governing enhanced performance, and the latest developments reported over the past few years. In addition, the current challenges and future research directions, including environmentally benign synthesis, improved oxidation stability, and computational materials design assisted by machine learning, are critically discussed to provide guidance for the rational development of next-generation $Ti_3C_2T_x$-based composites.

2. Synthesis strategies and properties

2.1. Synthesis of MXene

Two primary methods have been investigated for preparing MXene: top-down techniques and bottom-up approaches. The top-down methods involve etching the aluminum (Al) layer from MAX phase precursors to isolate MXene nanosheets. This approach offers several advantages over others, such as the ability to control the morphology, composition, and structure of MXenes, resulting in large surface areas. Additionally, it is considered more cost-effective and suitable for industrial-scale production compared to bottom-up methods. Various etchants have been employed to obtain $Ti_3C_2T_x$ MXene with precise stoichiometry and high purity, including molten salts, lithium fluoride (LiF), hydrochloric acid (HF), and hydrofluoric acid (HF). As shown in Figure 1a-b, the functional surface groups of MXene depend on the etchant used, which enhances its performance and facilitates its promising applications (Zhang et al. 2022, Chang and Xiao 2023, Iqbal et al. 2023, Lamiel et al. 2023, Li et al. 2024).

HF Etching:

Ti_3AlC_2, a common MAX phase, is frequently used to prepare $Ti_3C_2T_x$ MXene. The process involves slowly adding Ti_3AlC_2 into a 50% HF solution at 50 °C (Tran et al. 2021a). After 24 hours of reaction, multilayered $Ti_3C_2T_x$ MXene with a distinctive accordion-like morphology is formed. The Al layers are removed, leaving functional groups such as –F, –OH, and –O on the surface of the MXene. These multilayer structures are interconnected by hydrogen bonds and *Van Der Waals* forces. The concentration of HF significantly affects the quality of the MXene lamellas, with lower HF concentrations leading to reduced interlayer gaps.

Mechanical exfoliation techniques, such as high-power sonication and scotch tape exfoliation, are used to obtain few-layered MXene, though these methods introduce defects and reduce efficiency (Malaki et al. 2019, Zhang and Zhang 2022, Song et al. 2024). Inorganic cations such as NH_4^+, Na^+, and K^+ can also be employed for electrochemical delamination.

Acid/Fluoride Salt Etching:

In situ HF etching is a common method in the MXene preparation process, involving a mixture of fluoride salts and acids, such as HCl and LiF, LiF and NH_4F, or KF. These etchants allow the preparation of high-quality $Ti_3C_2T_x$ MXene with minimal defects through simple techniques like shaking and sonication. In situ HF etching has been investigated as a favorable alternative to concentrated HF, owing to its toxicity, environmental effects, and corrosiveness (Kagalkar et al. 2023, Htwe et al. 2024, Zhang et al. 2024).

The replacement of HF with a mixture of HCl and HF for MXene synthesis offers a safer, more ecologically friendly etching technique. These *in-situ* HF-etched MXenes exhibited superior electrochemical performance compared to HF-etched MXenes. This enhancement can be attributed to the doubling of electrochemical capacity and the presence of more –OH and –O functional groups relative to –F termination groups, which potentially enhance ion diffusion and improve ion transport characteristics. Additionally, the interlayer spacing between MXene layers can be increased, providing more space for ion transport (Kiran et al. 2024, Singh et al. 2025).

Electrochemical Etching:

In electrochemical etching, the MAX phase is immersed in an electrolyte solution that facilitates ion transport. An electric potential is applied across compatible anode and cathode electrodes to facilitate the electrochemical reaction, which removes the Al layers while preserving the MXene structures, due to the lower reactivity of the Ti-C bond compared to the Ti-Al bond. By adjusting the appropriate voltage between the cathode and anode, charges travel between the target material and the electrolyte, facilitating the etching process (Yin et al. 2021, Lim et al. 2022, Hao Ran Huang et al. 2025). For example, Jizhang *et al.* prepared F-free, Cl-containing MXenes using an electrolyte solution (LiOH + LiCl). After applying a constant voltage of 5.5 V for 5 hours, the $Ti_3C_2T_x$ layers were collected with a high efficiency of 92%. Li^+ ions participated in the etching process, expanding the interlayer spacing and facilitating the delamination process. This approach allows the MXene to achieve a lateral size of 3.8 µm and a thickness of approximately 4 nm. This efficient technique offers a time-saving process that is more facile compared to traditional etching methods (Chen et al. 2022).

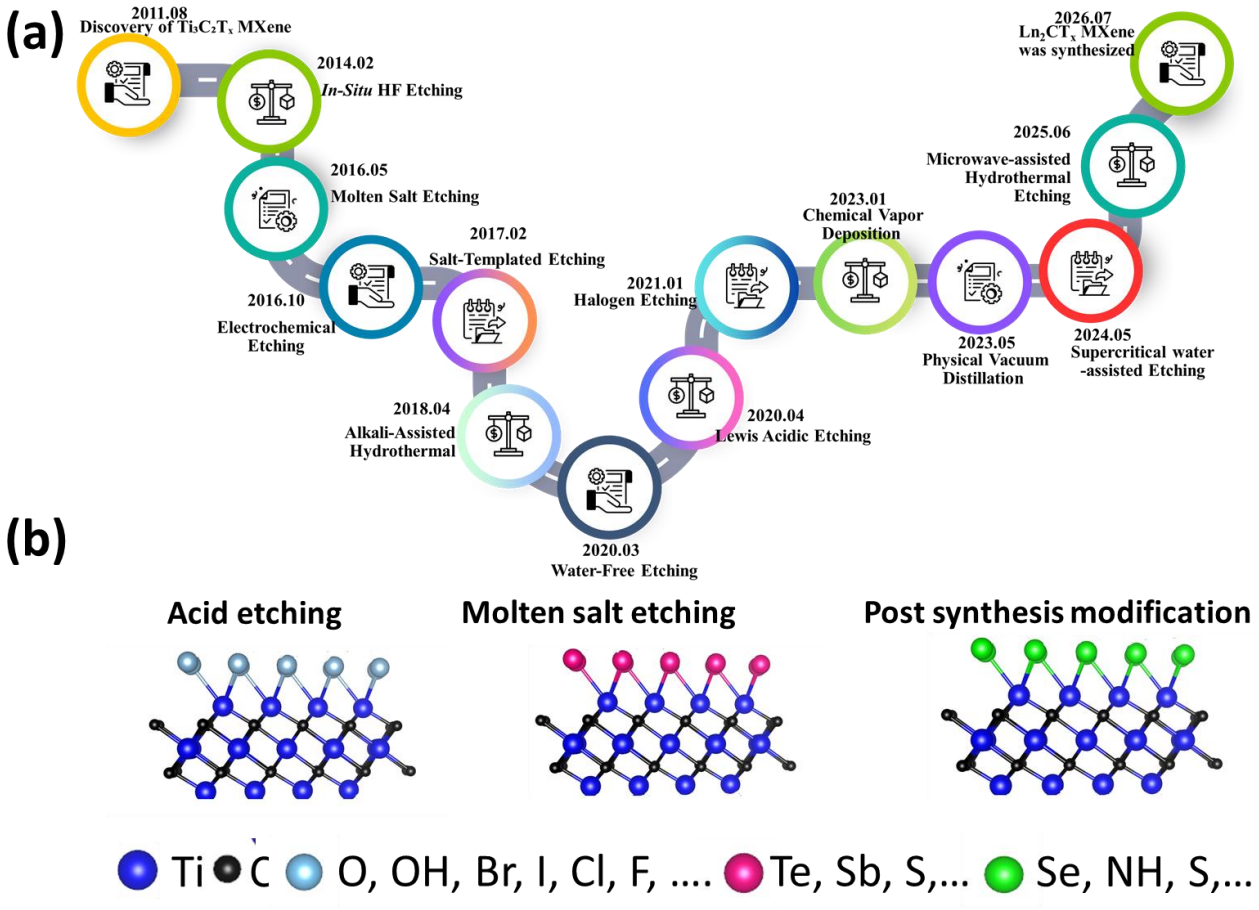

Figure 1. (a) Timeline summarizing the development of MXene synthesis methods since 2011, (b) surface functional group modification strategies for MXenes.

Molten Salt Etching

In the molten salt etching method, molten salt is used as the etchant to remove the Al layer in shorter reaction times, achieving F-free MXene in a controlled system without exposure to or extensive chemical intervention. For instance, Li and colleagues applied $ZnCl_2$ to prepare Cl-terminated MXenes at 550°C (Li et al. 2019). At high temperature, a substitution reaction occurs between Al and Zn^{2+}, leading to the occupation of Zn atoms in the A-sites of the MAX phase, thus creating a Zn-MAX phase prior to etching. This etching effect, facilitated by the Lewis acid properties of molten salts, offers a green and viable route for synthesizing F-free MXenes. In a similar approach, a mixture of Ti_3AlC_2:$CuCl_2$:NaCl:KCl was used to prepare MXenes under flowing Ar at 680 °C. It is believed that the molten salt facilitates the oxidation of Al to Al^{3+} and the reduction of Cu^{2+} to Cu during heat treatment. The sophisticated reaction is illustrated as follows (Pranada et al. 2025)

$$Ti_3AlC_2 + 1.5\ CuCl_2 \rightarrow Ti_3C_2 + AlCl_3 + 1.5\ Cu$$

$$Ti_3C_2 + 1.5\ CuCl_2 \rightarrow Ti_3C_2Cl_2 + Cu$$

A major drawback of the molten salt etching technique is that the resulting MXenes are typically difficult to delaminate into stable single-layer dispersions because of their limited hydrophilic surface terminations, which restricts their use in solution-processable applications such as inks and coatings.

Following the selective etching process, the as-synthesized MXenes typically exhibit a multilayered morphology. To fully exploit their unique physicochemical properties, these multilayered structures are subsequently exfoliated into single-layer or few-layer nanosheets through a process known as delamination. Delamination significantly increases the accessible surface area and exposes abundant active sites, thereby enhancing the performance of MXenes in a wide range of applications. The primary objective of the delamination process is to weaken the strong interlayer interactions between adjacent MXene sheets. This can be achieved through either mechanical or chemical approaches, including manual shaking, bath or probe sonication, and chemical intercalation using suitable guest species. Compared with their multilayer counterparts, delaminated MXenes exhibit colloidal stability, solvent dispersibility, high electrical conductivity, and enhanced electrochemical performance.

As shown in Figure 2, various organic molecules, such as dimethyl sulfoxide (DMSO), tetramethylammonium hydroxide (TMAOH), tetrabutylammonium hydroxide (TBAOH), and other organic amines, have been widely employed as intercalating agents during the delamination process. These molecules facilitate the expansion of the interlayer spacing, thereby promoting efficient exfoliation into single- or few-layer nanosheets. In addition to serving as effective intercalants, these solvents also improve the stability of MXene dispersions by suppressing nanosheet restacking and reducing oxidation during processing and storage. Without appropriate intercalation and stabilization, MXenes are highly susceptible to oxidation, leading to the formation of TiO_2 and amorphous or graphitic carbon, which deteriorates their electrical conductivity and structural integrity. Appropriate intercalating agents play a crucial role in preserving the physicochemical properties of MXenes and ensuring the long-term stability of MXene-based inks and solution-processed materials.

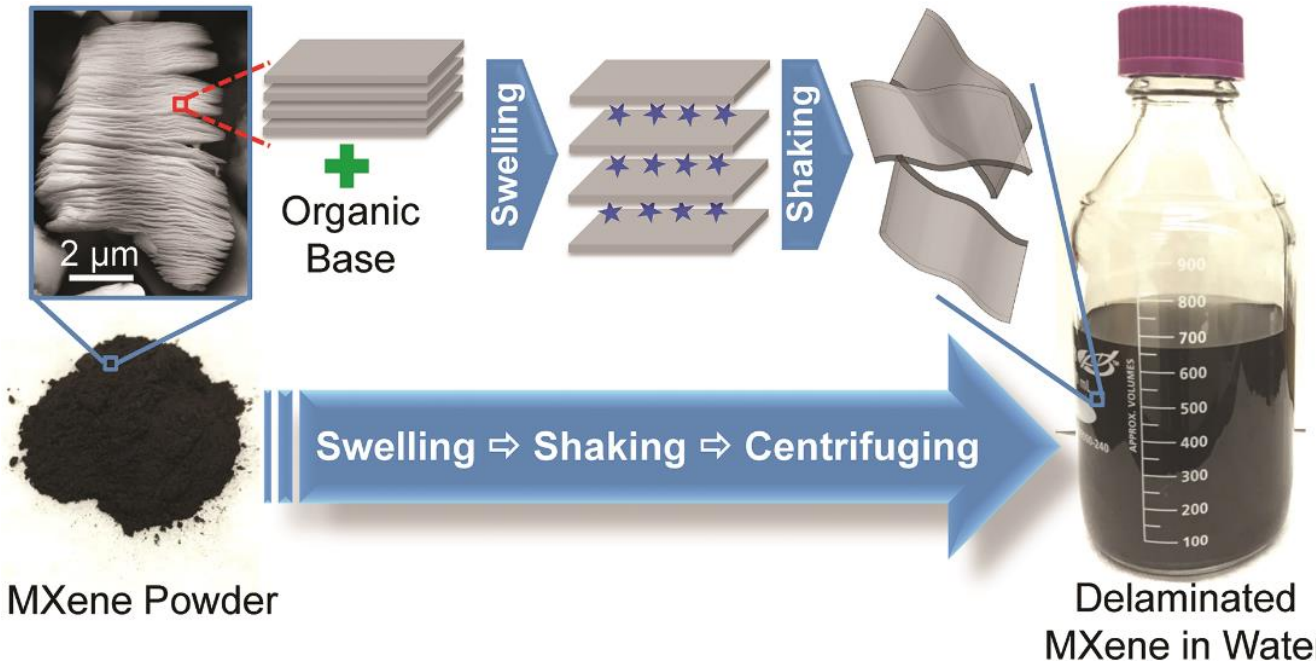

Figure 2. Schematic illustration of the preparation and delamination of multilayer MXene into few-layer MXene nanosheets. Reprinted and adapted with permission from Ref. (Naguib et al. 2015)

Although excessive –F terminations may reduce catalytic activity by blocking active sites and weakening reactant adsorption, HF-etched MXene exhibits high electrical conductivity and abundant surface functional groups, making it highly suitable for chemiresistive gas-sensing applications. In contrast, the acid/fluoride salt etching method typically produces larger MXene flakes

with fewer structural defects, higher electrical conductivity, and enhanced environmental stability compared with direct HF etching. Moreover, its lower fluorine content and facilitated intercalation process render the resulting MXenes more suitable for both gas sensing and catalytic applications. Owing to these advantages, acid/fluoride salt etching has become the most widely adopted synthesis strategy. In contrast, electrochemical etching offers a fluoride-free or low-fluoride route for MXene synthesis, enabling precise control over the surface chemistry. This method generally produces MXenes with a higher proportion of –O and –OH terminations, which serve as favorable active sites for CO_2 adsorption and activation. However, the electrical conductivity, structural quality, and production yield are highly dependent on the electrolyte composition and operating conditions. Similarly, molten salt etching produces fluoride-free or low-fluoride MXenes with tunable surface terminations and excellent thermal stability. The oxygen-rich surface chemistry generated by this method is particularly beneficial for catalytic processes, including CO_2 reduction. Nevertheless, molten salt etching remains relatively immature and has been less extensively explored for gas-sensing applications than conventional HF-based or acid/fluoride salt etching methods.

2.2. Properties

The mechanical, electrical and magnetic properties of $Ti_3C_2T_x$ MXene depend on the surface functionalization groups, which are influenced by the method and etchant used during the etching procedure. It is estimated that $Ti_3C_2O_x$ MXenes have significantly higher elastic stiffness compared to $Ti_3C_2OH_x$ and $Ti_3C_2F_x$ MXenes (Zhan et al. 2020). The termination groups act as a buffering factor for MXene under tensile deformation, inhibiting the collapse of the Ti layer and improving the critical strain ability at the point where the MXene fractures.

The mechanical properties of $Ti_3C_2T_x$ can be enhanced when combined with carbon materials or polymers. For instance, the tensile strength and flexibility of $Ti_3C_2T_x$-polyvinyl alcohol (PVA) heterostructures are four times greater than that of pure MXene. Moreover, $Ti_3C_2T_x$-polyacrylamide and $Ti_3C_2T_x$-polyethylene exhibit toughness and yield strength compared to their counterparts (Naguib et al. 2016, Zhang et al. 2016, Mayerberger et al. 2017). With an interpolation error of around 10%, the Young's modulus values, measured from the strain-stress properties, are 534, 502, and 597 GPa for $Ti_4C_3T_x$, $Ti_3C_2T_x$, and Ti_2CT_x MXenes, respectively. It is confirmed that the Young's modulus increases as the thickness of the MXene layers decreases (Borysiuk et al. 2015, Zha et al. 2015, Liu et al. 2016). The abundant functional groups on Mxene surface commonly brings the work functions (WFs) at intermediate value of wide range (1.8 eV ~ 8eV). The WFs increase with positive surface dipole moment in Ti_3C_2Ox in comparison with negative surface dipole moment in $Ti_3C_2OH_x$ and thus decreases WFs. On the other hand, the value of Ti_3C_2Fx usually fall between O-terminated MXene and OH-terminated MXene, therefore the control the functional groups are indispensable in understanding electrical properties (Lipatov and Sinitskii 2019, Tang et al. 2021, Wyatt et al. 2021, Ma et al. 2025). The Schottky barrier (SB) and van der Waals force were formed in MXene-based composite depending on WFs and Fermi level pinning. The low WFs of $Ti_3C_2T_x$ can enable the SB-free electron movement into the metal oxide semiconductor and vice versa. The n-type SB-free contacts between transition metal dichalcogenides and $Ti_3C_2OH_x$ with low WFs, which possess tremendous potential in nanoelectronics (Zhan et al. 2020).

Pristine $Ti_3C_2T_x$ is usually described as paramagnetic, or weakly ferrimagnetic, with the magnetic response shifting according to the etching procedure, defects, and surface terminations (Scheibe et al. 2019, Allen-Perry et al. 2021). Beyond these observations, extensive theoretical studies predict that MXenes can adopt both ferromagnetic and antiferromagnetic phases (Khazaei et al. 2013, Srivatsa et al. 2024, Yang et al. 2024). Such intrinsically magnetic MXenes are typically obtained by selective etching of the A element from MAX phases that are themselves predicted to be magnetic - for example, Cr_2AlC, Cr_2GeC (Jaouen et al. 2014), or by forming ordered double-transition-metal MXenes such as $Cr_2TiC_2T_x$ (Jaouen et al. 2014, Sun et al. 2018, Li et al. 2021). One study reported a paramagnetic to antiferromagnetic transition whose transition temperature depended on the chemical etching procedure (Allen-Perry et al. 2021), while another found that annealing of $Ti_3C_2T_x$-MXene above 773 K can induce ferromagnetism (Zhang et al. 2020), this has motivated further investigation of its magnetic behavior above room temperature (> 300 K) (Zhang et al. 2020). Incorporating Ni or Co raised the room temperature susceptibility by one to two orders of magnitude (Yang et al. 2024). Besides, Gd-doped MXene showed a high magnetic moment at room temperature with a stable ferromagnetic hysteresis loop (Rafiq et al. 2020). $Ti_3C_2T_x$ is therefore better regarded as a magnetically tunable host – its magnetism arising from defects, terminations, or compositional modification – rather than as an intrinsically magnetic material. In addition, the terminal groups ($–T_x$, such as –OH, –F, or –O) and intercalated water molecules make it highly hydrophilic, allowing for easy dispersion in water and facile self-assembly into thin-films (Kamal et al. 2025, Xiong et al. 2025). Table 1 summarizes the physicochemical properties of $Ti_3C_2T_x$ MXene reported in the literature. The reported values may vary depending on the synthesis method, surface terminations, degree of delamination, and measurement conditions.

Table 1. Summary of the physicochemical properties of $Ti_3C_2T_x$ MXene.

Category	Property	Typical values/Description
Chemical Stability	Oxidation sensitivity	Stable in mildly acidic and neutral media (Natu et al. 2018)
		Susceptible to oxidation in the presence of O_2, light, and high humidity (Khalid et al. 2025)
Adsorption Properties	Specific surface area & Adsorption sites	~10–100 $m^2 \cdot g^{-1}$ (Cai and Kim 2025)
		Surface Ti–O, Ti–OH functional groups, and structural defects (Swain et al. 2025)
Chemical Properties	Hydrophilicity & Chemical reactivity	Highly hydrophilic & readily oxidized, forming TiO_2 upon exposure to air or water (Lee et al. 2025)
	Redox activity	Mixed Ti^{4+}/Ti^{3+} surface oxidation states (Bhat et al. 2024)
Mechanical Properties	Young's modulus & Flexibility	~330 GPa & High flexibility; suitable for bendable and flexible films (Idumah 2023)
Electronic Properties	Electrical conductivity	~10^3–10^4 $S \cdot cm^{-1}$ (Qiao et al. 2021)
	Band structure	Metallic or semi-metallic, depending on surface terminations (Qiao et al. 2021)
	Work function	~4.6–5.2 eV, depending on surface terminations (Qiao et al. 2021)

3. Potential applications

3.1. Gas sensor

The abundant surface functional groups endow $Ti_3C_2T_x$ MXene with exceptional gas adsorption capability through both physisorption and chemisorption. Although pristine $Ti_3C_2T_x$ is intrinsically metallic rather than semiconducting, its gas sensing response frequently exhibits p-type-like characteristics, arising from direct charge transfer between adsorbed gas molecules and the MXene surface (Figure 3a). Upon adsorption at room temperature, gas molecules induce charge redistribution, thereby modulating the electrical conductivity of the MXene. Reducing gases, such as NH_3 and H_2, donate electrons to $Ti_3C_2T_x$, promoting electron–hole recombination and decreasing the hole carrier concentration, which leads to an increase in electrical resistance. Conversely, oxidizing gases (e.g., NO_2) withdraw electrons from the MXene surface, increasing the effective hole concentration and consequently decreasing the electrical resistance, as schematically illustrated in Figure 3.

Furthermore, surface terminal groups play a crucial role in determining the gas sensing performance of $Ti_3C_2T_x$ MXene by regulating the adsorption strength, charge transfer, and selectivity toward target gas molecules. Reducing gases such as NH_3 preferentially interact with oxygen-containing functional groups (e.g., –O and –OH) through hydrogen bonding and Lewis acid–base interactions, facilitating electron donation to the MXene surface. In contrast, oxidizing gases such as NO_2, owing to their strong electron-withdrawing nature, readily adsorb onto oxygen-terminated Ti sites and defect sites, where they act as electron acceptors, promoting charge transfer from the MXene to the adsorbed molecules. Therefore, the type, density, and distribution of surface functional groups strongly influence the sensing response, recovery characteristics, and gas selectivity of $Ti_3C_2T_x$-based sensors.

For instance, the p-type feature of the MXene sensor is facilitated during the etching process, where oxygen species are adsorbed on the surface and converted into a series of oxygen ion species. In air, the concentration of hole carriers increases due to electron abstraction, leading to the formation of a hole accumulation layer (HAL) on the surface. In the ammonia gas environment, the target gas is absorbed and releases electrons to the MXene surface, resulting in the narrowing of the HAL thickness and a decrease in conductivity. Simultaneously, the absorbed NH_3 and oxygen species also release electrons to the MXene surface. Moreover, the functional groups also participate in the sensing process through hydrogen bonding and charge transfer, creating an electron cloud around the N atoms. On the other hand, the hydrophilic nature of the MXene surface also supports the attraction of gas molecules through electrostatic interactions and polar gases (Mirzaei et al. 2024).

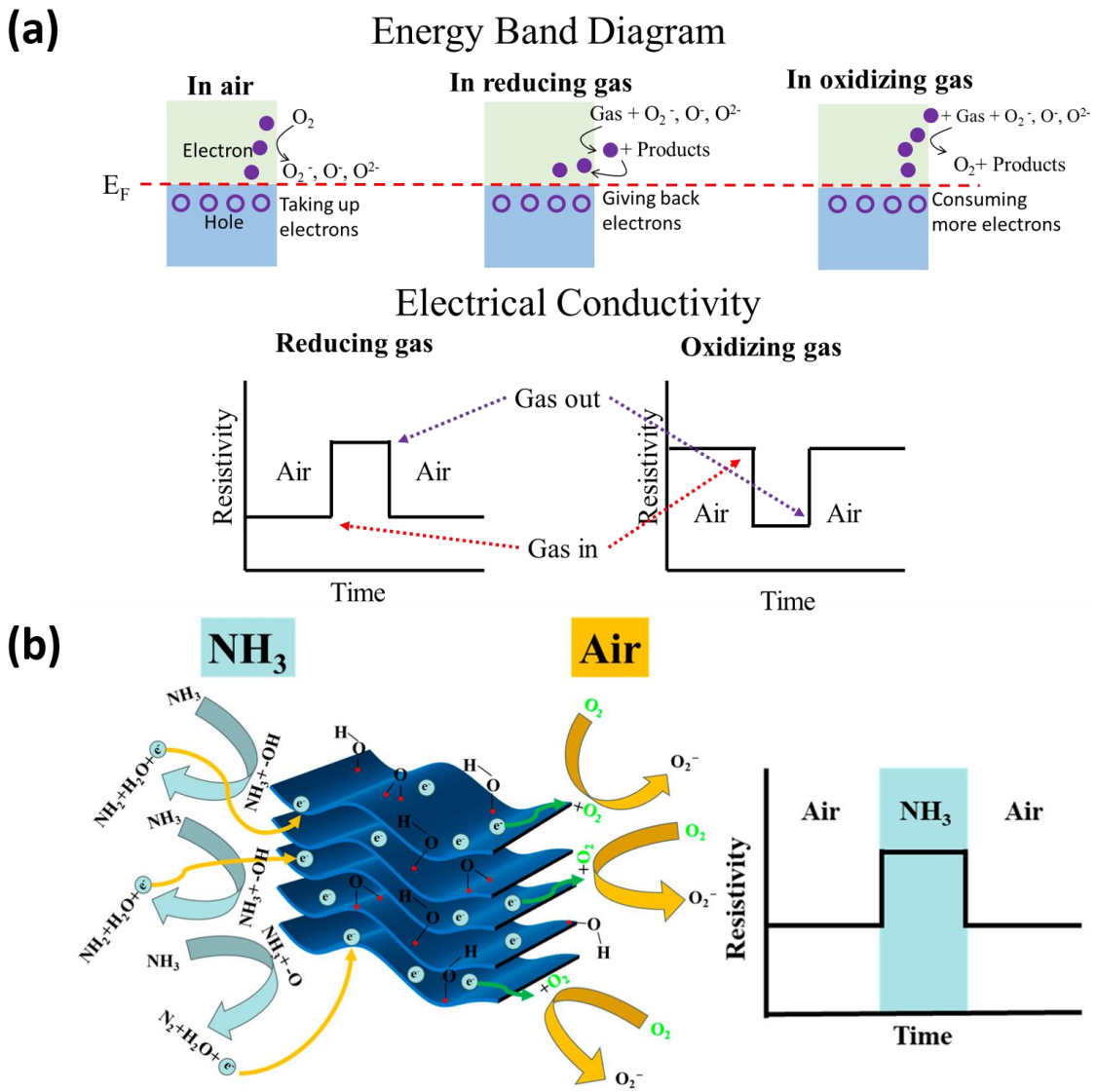

Figure 3. (a) Overall charge-transfer mechanism during gas sensing. (b) Surface adsorption mechanism of NH_3 on $Ti_3C_2T_x$ MXene. Reprinted and adapted with permission from Ref. (Tan et al. 2024) under CC BY 4.0.

The decoration of MoS_2 nanostructures on MXene exhibits performance in NH_3 detection at room temperature. The optimized composite shows better performance compared to pure MoS_2. The sensor demonstrates a high response (10%) when exposed to 100 ppm NH_3, with a quick response/recovery time (10/7 s). The improved gas sensor performance can be attributed to the formation of Schottky barriers between MoS_2 and MXene, which bend the MoS_2 energy band. The height of the Schottky barriers facilitates charge transfer due to the hydrogen bonding between NH_3 and MXene, which supports a stronger electron-donating effect (Guo et al. 2025). NaOH treatment increased the abundance of oxygen-containing functional groups on the MXene surface, which contributed to enhanced NH_3-sensing performance, yielding a high response of 100.3% with rapid response and recovery times of 73 and 38 s, respectively (Figure 4).

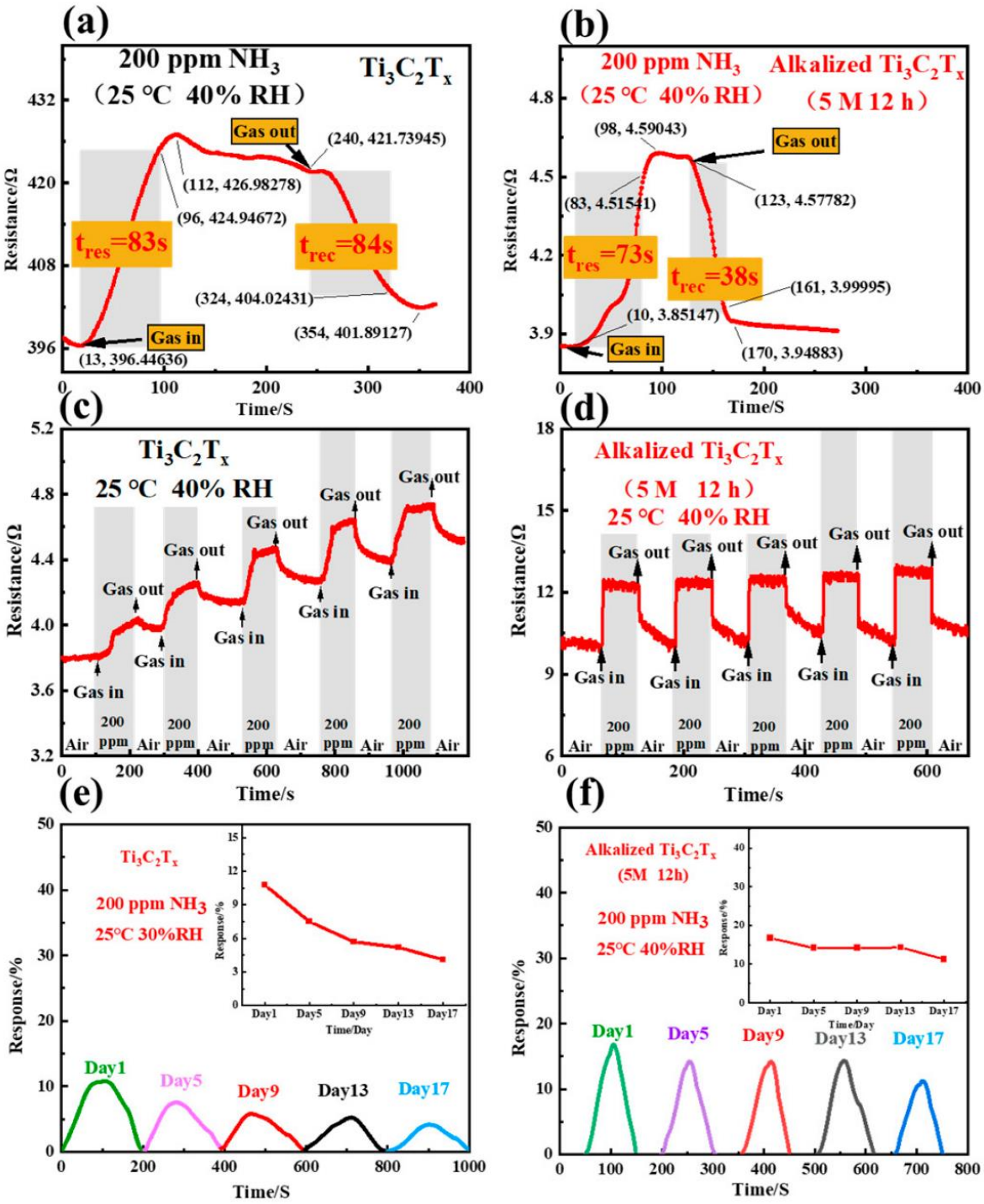

Figure 4. The NH_3 sensing of pristine and alkalized MXene. (a,b) Response and recovery characteristics to 200 ppm NH_3; (c,d) cyclic sensing responses; and (e,f) long-term stability over 17 days at 25 °C. Alkalized MXene was treated with 5 M KOH for 12 h. Reprinted and adapted from Ref. (Tan et al. 2024) under CC BY 4.0.

The p-n junction of $NiCo_2O_4$-MnO_2 was decorated onto multilayered $Ti_3C_2T_x$ MXene, which improved the detection of acetic acid at room temperature (Akhtar et al. 2025). The optimized composite exhibited a response (13%) to 20 ppm of acetic acid, with a detection limit of approximately 0.05 ppm at different relative humidities (25%, 50%, 70%, 95%). During the combination, Schottky barriers were formed, and the binding energy in the composite was distorted, facilitating the adsorption of oxygen molecules, which then converted into oxygen ions. The metallic conductivity of $Ti_3C_2T_x$ MXene provides a highly efficient electron transport network, enabling rapid carrier migration throughout the sensing material. This facilitates fast charge transfer following gas adsorption/desorption events, thereby substantially reducing the response and recovery times while enhancing the overall sensing performance. Furthermore, the electron affinity of oxygen (42 kJ/mol) is lower than that of acetic acid (327 kJ/mol), supporting the electron extraction process. Moreover, the abundance of functional groups and oxygen vacancies are key

factors that enhance the gas-sensing performance (Figure 5). Table 2 compares the room-temperature gas-sensing performance of various $Ti_3C_2T_x$-based gas sensors reported in the literature.

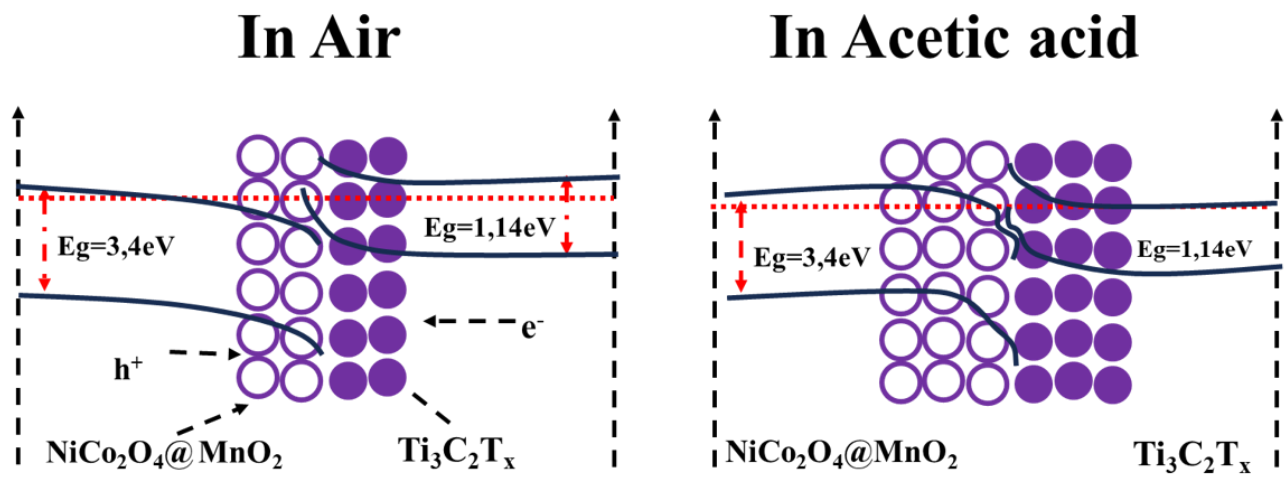

Figure 5. The sensing mechanism of acetic acid over $NiCo_2O_4$-MnO_2/MXene composites.

Table 2. Representative room-temperature gas-sensing performance of $Ti_3C_2T_x$-based gas sensors reported in the literature.

$Ti_3C_2T_x$-based gas sensors	Target Gas	Conc. (ppm)	Response/Recovery Time (s/s)	Response/ LOD	Ref.
$Ti_3C_2T_x$/rGO/CuO	Acetone	100	6.5/7.5	52.09%	(Liu et al. 2021)
Co_3O_4@PEI/$Ti_3C_2T_x$	NO_x	100	1.6/73.1	27.9%/30ppb	(Sun et al. 2021)
$Ti_3C_2T_x$	NH_3	100	1/201	28.87%	(Yang et al. 2019)
$Ti_3C_2T_x$/$Fe_2(MoO_4)_3$	N-butane	100	18/24	43.1%	(Zou et al. 2020)
$Ti_3C_2T_x$/WSe_2	Ethanol	40	9.7/6.6	24%	(Chen et al. 2020)
$Ti_3C_2T_x$/ZnO	NO_2	100	34/105	41.93%	(Yang et al. 2021)
$Ti_3C_2T_x$/MoS_2	Xylene	2.5	8/15	2.46Hz/1.23 ppm	(Samiei et al. 2026)

3.2. CO_2 reduction

Zero-dimensional $Ti_3C_2T_x$ MXene quantum dots (MQDs) are considered potential catalysts because of their unique features, including highly active sites and the quantum confinement effect. $Ti_3C_2T_x$ MQDs provide additional active sites through the edge effect, owing to their large specific surface area, while preventing light-shielding effects via abundant superficial functional groups. Their strong redox ability, resulting from a low Fermi level, also facilitates interfacial charge extraction, which is crucial for photocatalytic activity. Based on these favorable properties, $Ti_3C_2T_x$ MQDs were integrated with BiOI/g-C_3N_4 for photocatalytic CO_2 reduction at room temperature. The strong electron-withdrawing behavior of $Ti_3C_2T_x$ MQDs, combined with the internal electric field in BiOI/g-C_3N_4, forms a heterojunction photocatalyst for CO_2 photoreduction, resulting in a CO yield of 58 μmol g^{-1} h^{-1} and a CH_4 yield of 3.6 μmol g^{-1} h^{-1}, respectively. Under light illumination, CO_2 molecules are adsorbed onto the composite surface and react with superoxide radicals to convert into CO, as described in the following equation (Nie et al. 2025):

$$CO_2 \rightarrow *CO_2$$
$$H_2O + h^+ + e^- \rightarrow H^+ + OH^-$$
$$*CO_2 + e^- \rightarrow COO^-$$
$$COO^- + H^+ \rightarrow *COOH$$
$$*COOH + H^+ + e^- \rightarrow *CO$$
$$*CO + H^+ + e^- \rightarrow CHO* + CH_4$$

It is evident that the double heterojunction morphology of $Ti_3C_2T_x$ MXene and MOF-semiconductor facilitates dual high-speed electron separation through the synergistic effect of metallic MXene and the semiconductor. The 3MX-PEI-1/3-ZnO@Co_3O_4 composite demonstrates significantly improved CO_2 reduction performance, with CH_4 and CO reaction rates of approximately 43 and 596 μmol g^{-1} h^{-1}, respectively, along with high selectivity (6.7% for CH_4 and 93% for CO). CO_2 photoreduction depends on promoting C–O cleavage and H_2O dissociation at surface-active sites, which are influenced by repulsive forces and the high surface diffusion activation energy of adsorbed CO_2 molecules. Under ambient conditions, this increases surface mobility and enhances product formation.

As shown in Figure 6, electrons migrate from ZnO to $Ti_3C_2T_x$ MXene due to the fact that the conduction band (CB) edge of ZnO is higher than the Fermi level of $Ti_3C_2T_x$, which holds and prevents electron recombination at the ZnO sites. Moreover, the work function of MXene is higher than that of ZnO and Co_3O_4, causing the energy band to shift upwards and leading to the formation of a depletion layer. The high electron density from the d-electrons of the Ti layer forms a built-in electric field, supporting strong reduction and oxidation reactions of CO_2 under light illumination (Hou et al. 2024).

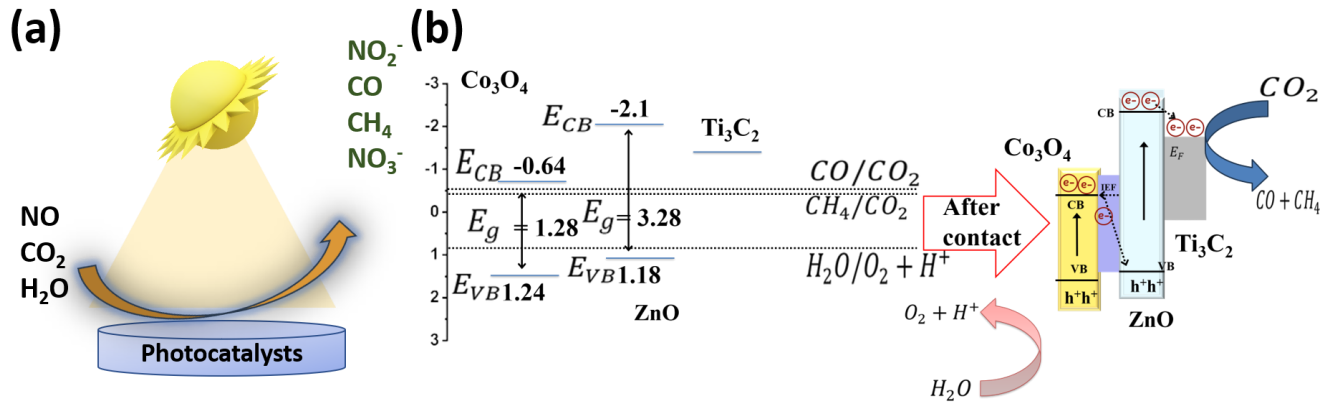

Figure 6. (a,b) The plausible mechanism for improved CO_2 photoreduction over double heterojunction.

Although there have been numerous experiments to confirm the properties of $Ti_3C_2T_x$ MXenes, a complete understanding of the plethora of functional groups, symmetry, and experimental procedures involved with MXenes still remains elusive. Computational methods and machine learning could help establish correlations between their properties and predict different composites with several orders of magnitude of accuracy, saving time and providing fundamental information for experimental analysis. In fact, machine learning has been extensively applied in materials informatics to analyze data collected from $Ti_3C_2T_x$ MXene. It offers a platform for pattern recognition, analysis, and prediction based on algorithms, with provisions for customization. The stability, cytotoxicity, and physicochemical properties of new MXenes were predicted to estimate the complex relationships in skin-like MXene electrodes.

$Ti_3C_2T_x$/PDMS sound detector was applied to the vibrating membrane of the speaker system, which recorded the resistance changes with short and long vowels. The training dataset was used as input for the syllable recognition convolutional-neural-network (SR-CNN) model, which demonstrates that as the number of training epochs increases, the accuracy of the training set improves (Jin et al. 2020). As shown in Figure 7, the X-axis represents the number of training epochs with iterations of the input values, while the Y-axis illustrates the recognition accuracy, which stabilizes around 95%. This confirms the effectiveness of the network's training at high accuracy. The loss function is depicted in Figure 7c, where the loss function increases linearly as the number of training epochs decreases. From the obtained values, the black and red dots are concentrated and scattered in a narrow region, indicating that the SR-CNN plays an important role in recognition. Therefore, the deep-learning-enabled $Ti_3C_2T_x$-based composite artificial throat sensor can be used to predict different pronunciations as a wearable device, supporting patients in communication.

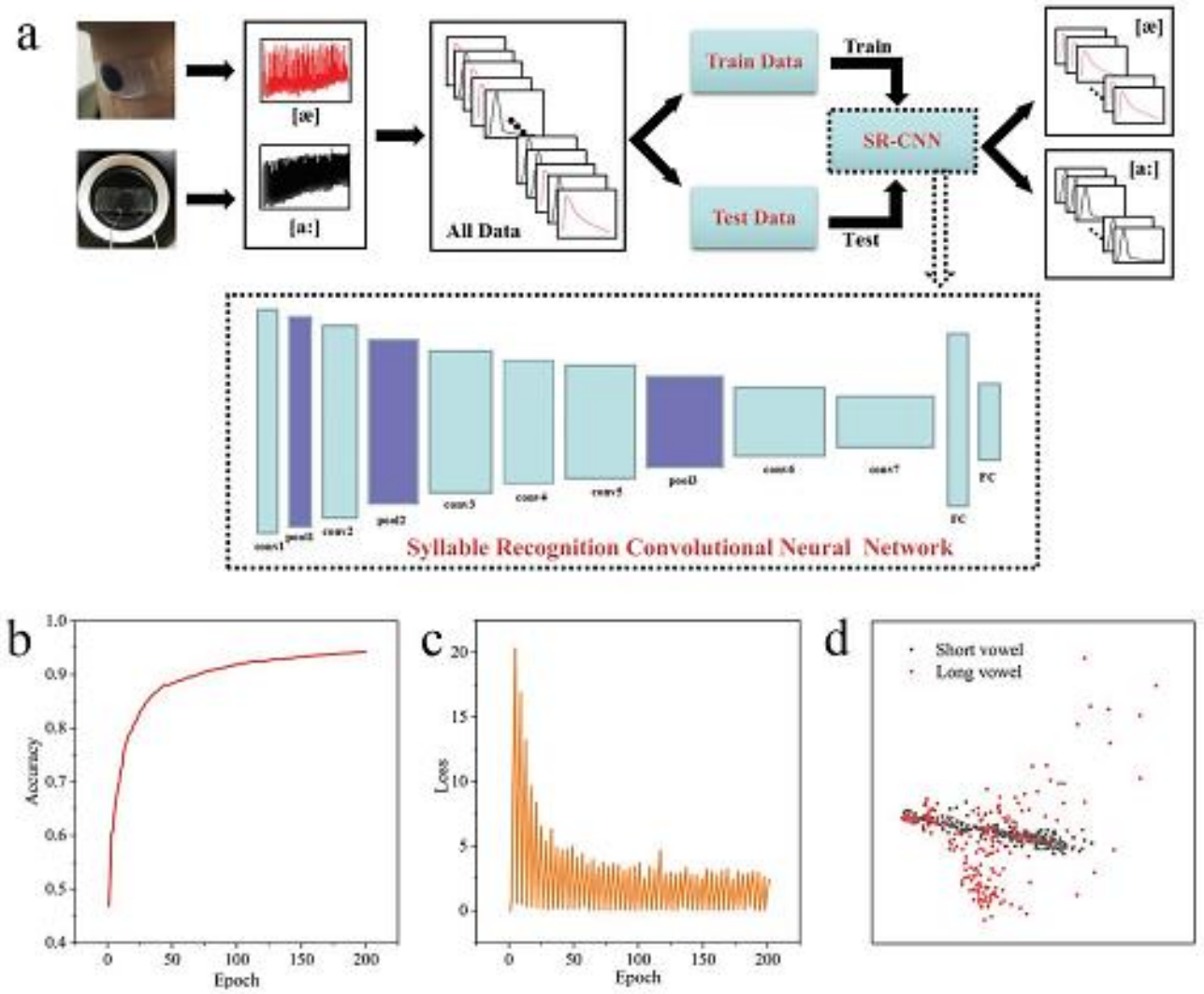

Figure 7. (a-d) Speech recognition over $Ti_3C_2T_x$/PDMS composite and deep-learning. Reprinted and adapted with permission from Ref. (Jin et al. 2020)

3.3. Other applications

In addition to gas sensing and CO_2 reduction, MXene-based composites have attracted considerable attention for a wide range of energy-related applications, particularly hydrogen evolution reaction (HER) electrocatalysis and interfacial solar steam generation, owing to their tunable electronic structure, high electrical conductivity, and excellent interfacial properties (Arshad et al. 2023, Irshad et al. 2023, 2025b, 2025a, Ali et al. 2025). For instance, CeO_2 was integrated with MXene to develop efficient electrocatalysts for the alkaline HER. Both in situ and ex situ hydrothermal synthesis routes were employed to investigate the influence of cerium precursors on the structural characteristics, active-site distribution, and electrocatalytic performance of the resulting composites. The results demonstrated that the composites prepared via the in situ hydrothermal method exhibited superior HER activity, delivering a low overpotential of approximately 54.4 mV at a current density of 10 mA cm^{-2}. This enhanced electrocatalytic performance was attributed to the strong interfacial coupling between CeO_2 and MXene, which promoted charge transfer, increased the density of accessible active sites, and optimized the electronic structure, thereby accelerating the HER kinetics under alkaline conditions (Huynh et al. 2026).

MXene has also been extensively explored for interfacial solar steam generation owing to its photothermal conversion capability (Irshad et al. 2023, 2025a, 2025b, Ali et al. 2025). To improve its oxidation resistance under high-humidity conditions, perovskite-type oxides were introduced as protective layers. The optimized composite achieved a high evaporation rate of 1.98 kg m^{-2} h^{-1} under one-sun illumination (Arshad et al. 2023). This remarkable performance was attributed to the porous structure and interconnected hydrogel architecture, which enhanced water transport, facilitated vapor escape, and improved mechanical stability during repeated wet–dry cycling under continuous solar irradiation. Furthermore, spinel $CoMn_2O_4$ and poly(vinyl alcohol) have also been incorporated into MXene-based structures to enhance solar steam generation efficiency. The performance

of these hybrid composites originates from their efficient photothermal conversion of incident solar energy into localized thermal energy, together with effective phonon scattering that suppresses heat dissipation. The optimized composite exhibited a low thermal conductivity of approximately 0.0822 ± 0.00394 W m^{-1} K^{-1}, thereby maximizing heat localization and promoting efficient steam generation (Alomar et al. 2026).

Besides experimental investigations, first-principles calculations were employed to elucidate the effect of Se and S doping on the structural and electronic properties of Ti_2CO_2 MXene for lithium–sulfur battery applications. The results demonstrated that pristine Ti_2CO_2 MXene exhibits weaker binding affinity toward Li_2S_x clusters than Se- and S-doped Ti_2CO_2 MXene. This enhancement is attributed to the hybridization between the dopant *p* orbitals and the Ti 3*d* orbitals, which strengthens the interaction with lithium polysulfides. Furthermore, the improved charge transport within the doped MXene enhances both the adsorption energy of Li_2S_x species and the electrical conductivity, thereby contributing to superior electrochemical performance in lithium–sulfur batteries (Chaudhary et al. 2021, Nguyen et al. 2025, Sheoran et al. 2025).

4. Current Challenges and Future Perspectives

Despite the remarkable advances in $Ti_3C_2T_x$-based composites, several critical challenges should be addressed before their large-scale production, and practical implementation can be realized.

(i) Development of green and scalable synthesis strategies.

The synthesis of high-quality $Ti_3C_2T_x$ MXenes remains highly dependent on HF or *in situ* HF etching, which poses significant health, safety, and environmental concerns because of the highly corrosive and toxic nature of fluoride-containing reagents. Although alternative approaches, including molten salt etching, electrochemical etching, hydrothermal-assisted etching, and halogen-assisted methods, have emerged as safer and more environmentally benign routes, they often suffer from relatively high processing costs, complex operating conditions, limited scalability, or insufficient control over MXene quality and surface chemistry. Therefore, developing fluorine-free, cost-effective, and scalable synthesis strategies capable of producing high-quality MXenes with controllable surface terminations remains a major research priority.

(ii) Oxidation stability and long-term durability.

Another major challenge is the poor oxidation stability of $Ti_3C_2T_x$ MXenes under ambient conditions, particularly in humid and oxygen-rich environments. Oxidation gradually converts $Ti_3C_2T_x$ into TiO_2 and amorphous or graphitic carbon, resulting in deterioration of electrical conductivity, structural integrity, and functional performance. Although several strategies, including low-temperature storage, antioxidant treatment, surface passivation, polymer encapsulation, and protective coatings, have been proposed to suppress oxidation, maintaining long-term stability without compromising the intrinsic properties of MXenes remains a significant challenge. Future studies should therefore focus on developing effective stabilization strategies that ensure long-term operational reliability under practical working conditions.

(iii) Precise control of surface functional groups and reproducibility.

The surface chemistry of $Ti_3C_2T_x$ MXenes is highly dependent on the synthesis route and processing conditions. The relative proportions of terminal groups (e.g., –O, –OH, –F, and –Cl) vary considerably with the choice of etchant, reaction temperature, and post-treatment procedures. Consequently, achieving precise control over the type, density, and spatial distribution of surface functional groups remains challenging. This variability also contributes to batch-to-batch inconsistencies in physicochemical properties and device performance. Establishing standardized synthesis protocols together with quantitative characterization techniques for surface terminations is therefore essential for improving reproducibility and enabling rational structure–property engineering.

(iv) Large-scale production, economic feasibility, and environmental sustainability.

Although laboratory-scale synthesis of $Ti_3C_2T_x$ MXenes has been extensively demonstrated, translating these processes to industrial-scale manufacturing remains challenging. The high cost of MAX-phase precursors, hazardous chemical consumption, multiple purification steps, and relatively low production efficiency all contribute to the overall manufacturing cost. In addition, effective treatment and recycling of fluoride-containing wastewater and other chemical by-products are essential to minimize environmental impacts and comply with sustainable manufacturing practices. Future efforts should therefore focus on developing continuous production processes, reducing synthesis costs, improving batch-to-batch consistency, and implementing environmentally responsible waste management strategies to facilitate the commercialization of MXene-based technologies.

5. Conclusions

In summary, $Ti_3C_2T_x$ MXenes have emerged as one of the most promising two-dimensional materials owing to their outstanding physicochemical properties, including metallic conductivity, tunable surface chemistry, large specific surface area, abundant surface functional groups, and hydrophilicity. These unique characteristics make $Ti_3C_2T_x$ an attractive platform for constructing high-performance composites for applications in photocatalysis, energy storage, and sensing. In photocatalytic systems, the performance of $Ti_3C_2T_x$-based composites is primarily attributed to efficient charge separation and transport, optimized interfacial contact, and the synergistic interactions between MXenes and semiconductor counterparts.

Despite these significant advances, several critical challenges remain before the widespread practical implementation of $Ti_3C_2T_x$-based materials can be realized. First, the development of environmentally friendly and fluorine-free etching strategies represents a key research priority to replace hazardous HF-based synthesis while maintaining high structural quality and controllable surface terminations. Second, the long-term oxidation stability of $Ti_3C_2T_x$, particularly in aqueous environments, remains one of the most significant obstacles limiting its practical applications. Future efforts should therefore focus on effective surface passivation, protective coatings, and rational interface engineering to suppress oxidation without compromising electrical conductivity or catalytic activity. Furthermore, precise control and quantitative characterization of surface functional groups are essential for establishing clear structure–property relationships and enabling the rational design of MXene-based materials with tailored functionalities.

Looking forward, the integration of advanced computational approaches, including density functional theory, molecular dynamics, and machine learning, is expected to play an increasingly important role in accelerating MXene research. These techniques can facilitate the prediction of thermodynamic stability, electronic structure, surface reactivity, and interfacial interactions, while enabling high-throughput screening of yet-to-be-synthesized MXene compositions and composite architectures. The combination of computational materials design with experimental validation is anticipated to significantly accelerate the discovery of next-generation $Ti_3C_2T_x$-based composites with enhanced stability, functionality, and application-specific performance.

References

Ajmal Z, Hayat A, Qadeer A, Zhao Y, Ibrahim EH, Haq M ul, Iqbal K, Imran M, Kuku M, Hussain I, Ali H, Orooji Y, Zhou JL, Ben T (2025) Advancements in MXene-based frameworks towards photocatalytic hydrogen production, carbon dioxide reduction and pollutant degradation: Current challenges and future prospects. Coordination Chemistry Reviews 523: 216226. https://doi.org/10.1016/J.CCR.2024.216226

Akhtar A, Sadaf S, Zhou R, Ling Q, Luo S, Han M, Di W, Liu J, Chen D, Chu X (2025) Highly responsive and stable room temperature acetic acid gas sensor based on nano-composite of MXene $Ti_3C_2T_x$-$NiCo_2O_4$-MnO_2. Journal of Alloys and Compounds 1010: 177715. https://doi.org/10.1016/J.JALLCOM.2024.177715

Alhabeb M, Maleski K, Anasori B, Lelyukh P, Clark L, Sin S (2017) Guidelines for Synthesis and Processing of Two-Dimensional Titanium Carbide ($Ti_3C_2T_x$ MXene). Chemistry of Materials 29: 7633-7644. https://doi.org/10.1021/acs.chemmater.7b02847

Ali MA, Irshad MS, Maqsood G, Arshad N, Aslam N, Asghar MS, Shakoor B, Hussain I, Younes MH, Mei T, Dao VD, Wang X (2025) Advances in flat-band structures for enhanced photothermal conversion efficiency: Design, mechanism, and complementary applications. Nano Energy 142: 111297. https://doi.org/10.1016/J.NANOEN.2025.111297

Allen-Perry K, Straka W, Keith D, Han S, Reynolds L, Gautam B, Autrey DE (2021) Tuning the Magnetic Properties of Two-Dimensional MXenes by Chemical Etching. Materials 14: 694. https://doi.org/10.3390/MA14030694

Alomar M, El Maati LA, Irshad MS, Arshad N, Alotaibi A, Mushtaq N, Dao VD, Wang X (2026) 3D photothermal hydrogels derived from spinel $CoMn_2O_4$@MXene nanocomposites for an efficient solar-driven evaporation system. RSC Advances 16: 17522–17535. https://doi.org/10.1039/d6ra00897f

Anasori B, Gogotsi Y (2023) The global expansion of MXenes. Graphene and 2D Materials 8: 39–41. https://doi.org/10.1007/s41127-023-00067-1

Anasori B, Lukatskaya MR, Gogotsi Y (2017) 2D metal carbides and nitrides (MXenes) for energy storage. Nature Reviews Materials 2: 16098. Available from: http://dx.doi.org/10.1038/natrevmats.2016.98.

Arshad N, Irshad MS, Asghar MS, Alomar M, Tao J, Shah MAKY, Wang X, Guo J, Wageh S, Al-Hartomy OA, Kalam A, Hao Y, Ouyang Z, Zhang H (2023) 2D MXenes Embedded Perovskite Hydrogels for Efficient and Stable Solar Evaporation. Global Challenges 7: 2300091. https://doi.org/10.1002/GCH2.202300091

Ayodhya D (2023) A review of recent progress in 2D MXenes: Synthesis, properties, and applications. Diamond and Related Materials 132: 109634. https://doi.org/10.1016/j.diamond.2022.109634

Barsoum MW, Gogotsi Y (2023) Removing roadblocks and opening new opportunities for MXenes. Ceramics International 49: 24112–24122. https://doi.org/10.1016/j.ceramint.2022.10.051

Benchakar M, Loupias L, Garnero C, Bilyk T, Morais C, Canaff C, Guignard N, Morisset S, Pazniak H, Hurand S (2020) One MAX phase, different MXenes: A guideline to understand the crucial role of etching conditions on $Ti_3C_2T_x$ surface chemistry. Applied Surface Science 530: 147209. https://doi.org/10.1016/j.apsusc.2020.147209

Bhat MY, Adeosun WA, Prenger K, Samad YA, Liao K, Naguib M, Mao S, Qurashi A (2024) Frontiers of MXenes-based hybrid materials for energy storage and conversion applications. Advanced Composites and Hybrid Materials 8: 52. https://doi.org/10.1007/S42114-024-01121-Z

Borysiuk VN, Mochalin VN, Gogotsi Y (2015) Molecular dynamic study of the mechanical properties of two-dimensional titanium carbides $Ti_{n+1}C_n$ (MXenes). Nanotechnology 26: 265705. https://doi.org/10.1088/0957-4484/26/26/265705

Cai Z, Kim H (2025) Recent advances in MXene gas sensors: synthesis, composites, and mechanisms. npj 2D Materials and Applications 9: 66. https://doi.org/10.1038/s41699-025-00586-w

Chang L, Xiao X (2023) The review of MXenes for osmotic energy harvesting: Synthesis and properties. Diamond and Related Materials 136: 109971. https://doi.org/10.1016/j.diamond.2023.109971

Chaudhary S, Raja M, Sinha OP (2021) A review on the different types of electrode materials for aqueous supercapacitor applications. Advances in Natural Sciences: Nanoscience and Nanotechnology 12: 015011. https://doi.org/10.1088/2043-6262/ABE93E

Chen J, Chen M, Zhou W, Xu X, Liu B, Zhang W, Wong C (2022) Simplified Synthesis of Fluoride-Free $Ti_3C_2T_x$ via Electrochemical Etching toward High-Performance Electrochemical Capacitors. ACS Nano 16 (2): 2461–2470. https://doi.org/10.1021/acsnano.1c09004

Chen WY, Jiang X, Lai SN, Peroulis D, Stanciu L (2020) Nanohybrids of a MXene and transition metal dichalcogenide for selective detection of volatile organic compounds. Nature Communications 11: 1302. https://doi.org/10.1038/s41467-020-15092-4

Ghanbari R, Wu D, Heynderickx PM (2025) Fabrication of MXene-based membranes and their application in per- and polyfluorinated substances removal: Comparison with commercial membranes, challenges, and future improvements. Coordination Chemistry Reviews 523: 216253. https://doi.org/10.1016/J.CCR.2024.216253

Gogotsi Y (2023) MXenes: From Discovery to Applications of Two-Dimensional Metal Carbides and Nitrides. CRC Press. https://doi.org/10.1201/9781003306511

Gogotsi Y, Huang Q (2021) MXenes: two-dimensional building blocks for future materials and devices. ACS nano 15: 5775–5780. https://doi.org/10.1021/acsnano.1c03161

Guo Z, Zhang H, Zhang J, Alwadie N, Duan L, Li Y, Hou Z, Dao VD, Irshad MS (2025) Tailoring MoS_2 nanoflakes over MXenes nanobelts for efficient ammonia detection at room temperature. Journal of Alloys and Compounds 1010: 177710. https://doi.org/10.1016/J.JALLCOM.2024.177710

Hao Ran Huang J, Tseng SW, Peter Chen IW (2025) In-situ electrochemical XRD and raman probing of ion transport dynamics in ionic liquid-etched $Ti_3C_2T_x$ MXene for energy storage applications. Chemical Engineering Journal 503: 158232. https://doi.org/10.1016/J.CEJ.2024.158232

Hou X, Zhang Z, Ma Z, Gao X, Wang H, Jia L (2024) Enhancing CO_2 photoreduction efficiency with MXene-modified ZnO@Co_3O_4 double heterojunction. Chemical Engineering Journal 500: 157158. https://doi.org/10.1016/J.CEJ.2024.157158

Htwe YZN, Bakar SA, Mohamed A, Muqoyyanah, Othman MHD, Mamat MH, Ahmad MK, Azis MNA, Nuryadi R, Ramakrishna S, Salah N, Alshahrie A (2024) Progress in etching-driven MXene synthesis and utilization in conductive inks for printed electronics applications: A comprehensive review. Synthetic Metals 306: 117631. https://doi.org/10.1016/J.SYNTHMET.2024.117631

Huynh NHT, Tien VM, Thanh LT, Pham HTQ, Huynh STM, Huynh TT, Pham HQ (2026) Effect of in-situ/ex-situ hydrothermal routes on electrocatalytic hydrogen evolution performance of CeO_2/N-$Ti_3C_2T_x$ composites. Advances in Natural Sciences: Nanoscience and Nanotechnology 17: 035001. https://doi.org/10.1088/2043-6262/AE8A56

Idumah CI (2023) MXene polymeric nanoarchitectures mechanical, deformation, and failure mechanism: A review. Polymer-Plastics Technology and Materials 62: 443–466. https://doi.org/10.1080/25740881.2022.2114365

Ighalo JO, Rangabhashiyam S, Adeyanju CA, Ogunniyi S, Adeniyi AG, Igwegbe CA (2022) Zeolitic Imidazolate Frameworks (ZIFs) for aqueous phase adsorption – A review. Journal of Industrial and Engineering Chemistry 105: 34–48. https://doi.org/10.1016/J.JIEC.2021.09.029

Iqbal A, Hassan T, Gao Z, Shahzad F, Koo CM (2023) MXene-incorporated 1D/2D nano-carbons for electromagnetic shielding: a review. Carbon 203: 542-560. https://doi.org/10.1016/j.carbon.2022.11.104

Irshad MS, Arshad N, Asghar MS, Hao Y, Alomar M, Zhang S, Zhang J, Guo J, Ahmed I, Mushtaq N, Shah MAKY, Noureen L, Wageh S, Al-Hartomy OA, Kalam A, Dao VD, Wang H, Wang X, Zhang H (2023) Advances of 2D-Enabled Photothermal Materials in Hybrid Solar-Driven Interfacial Evaporation Systems toward Water-Fuel-Energy Crisis. Advanced Functional Materials 33: 2304936. https://doi.org/10.1002/ADFM.202304936

Irshad MS, Arshad N, Maqsood G, Asghar MS, Wu P, Mushtaq N, Shah MAKY, Lin L, Li X, Ahmed I, Mei T, Sabir M, Wang H, Pham P V, Li H, Nang HX, Dao VD, Guo J, Wang X (2025a) Interdisciplinary Hybrid Solar-Driven Evaporators: Theoretical Framework of Fundamental Mechanisms and Applications. Small 21: 2407280. https://doi.org/10.1002/SMLL.202407280

Irshad MS, Arshad N, Maqsood G, Ahmed I, Shakoor B, Asghar MS, Ghazanfar U, Lin L, Shah MAKY, Ahmed I, Chen X, Wang J, Yi C, Li J, Qian J, Li W, Said Z, Li H, Ho NX, Wang H, Fan X, Mushtaq N, Dao VD, Mei T, Wang X (2025b) Advancing water collection efficiency in hybrid solar evaporators: key factors, strategic innovations, and synergistic applications. Materials Science and Engineering: R: Reports 165: 101018. https://doi.org/10.1016/J.MSER.2025.101018

Jaouen M, Bugnet M, Jaouen N, Ohresser P, Mauchamp V, Cabioc'H T, Rogalev A (2014) Experimental evidence of Cr magnetic moments at low temperature in Cr_2A(A=Al,Ge)C. Journal of Physics: Condensed Matter 26: 176002. https://doi.org/10.1088/0953-8984/26/17/176002

Jin Y, Wen B, Gu Z, Jiang X, Shu X, Zeng Z, Zhang Y, Guo Z, Chen Y, Zheng T, Yue Y, Zhang H, Ding H (2020) Deep-Learning-Enabled MXene-Based Artificial Throat: Toward Sound Detection and Speech Recognition. Advanced Materials Technologies 5: 2000262. https://doi.org/10.1002/ADMT.202000262

Kagalkar A, Dharaskar S, Chaudhari N (2023) 2D-Transition Metal Carbides and Nitrides: Prospects and Challenges. ACS Symposium Series 1445: 1–42. https://doi.org/10.1021/BK-2023-1445.CH001

Kamal A, Li B, Luo S, Kinloch I, Zheng L, Liao K (In press) Engineering the mechanical properties of $Ti_3C_2T_x$ MXene films via thermal annealing treatment. Nano Materials Science. https://doi.org/10.1016/J.NANOMS.2025.03.006

Khalid Z, Hadi F, Xie J, Chandrabose V, Oh JM (2025) The Future of MXenes: Exploring Oxidative Degradation Pathways and Coping with Surface/Edge Passivation Approach. Small 21: 2407856. https://doi.org/10.1002/SMLL.202407856

Khazaei M, Arai M, Sasaki T, Chung CY, Venkataramanan NS, Estili M, Sakka Y, Kawazoe Y (2013) Novel electronic and magnetic properties of two-dimensional transition metal carbides and nitrides. Advanced Functional Materials 23: 2185–2192. https://doi.org/10.1002/ADFM.201202502

Kiran NU, Soren S, Chatterjee S, Besra L (2024) Synthesis and characterization of MXenes through an array of conventional methods and green synthesis routes. In: Chakroborty S (Ed.) MXenes: From Research to Emerging Applications. CRC Press, Boca Raton, 11–28. https://doi.org/10.1201/9781003366225-2

Lamiel C, Hussain I, Warner JH, Zhang K (2023) Beyond Ti-based MXenes: A review of emerging non-Ti based metal-MXene structure, properties, and applications. Materials Today 63: 313–338. https://doi.org/10.1016/j.mattod.2023.01.020

Lee S, Yang E, Lee J, Ko TY, Kim SJ (2025) Covalent Surface Modification of Hydrophobic Alkoxides on $Ti_3C_2T_x$ MXene Nanosheets Toward Amphiphilic and Electrically Conductive Inks. Advanced Materials 37: 2502440. https://doi.org/10.1002/ADMA.202502440

Lehman JH, Terrones M, Mansfield E, Hurst KE, Meunier V (2011) Evaluating the characteristics of multiwall carbon nanotubes. Carbon 49: 2581–2602. https://doi.org/10.1016/J.CARBON.2011.03.028

Li J, Chen X, Zhu X, Jiang Y, Chang X, Sun S (2024) Two-dimensional transition metal MXene-based gas sensors: A review. Chinese Chemical Letters 35: 108286. https://doi.org/10.1016/j.cclet.2023.108286

Li M, Lu J, Luo K, Li Y, Chang K, Chen K, Zhou J, Rosen J, Hultman L, Eklund P, Persson POÅ, Du S, Chai Z, Huang Z, Huang Q (2019) Element Replacement Approach by Reaction with Lewis Acidic Molten Salts to Synthesize Nanolaminated MAX Phases and MXenes. Journal of the American Chemical Society 141: 4730–4737. https://doi.org/10.1021/JACS.9B00574

Li S, He J, Grajciar L, Nachtigall P (2021) Intrinsic valley polarization in 2D magnetic MXenes: surface engineering induced spin-valley coupling. Journal of Materials Chemistry C 9: 11132–11141. https://doi.org/10.1039/D1TC02837E

Lim KRG, Shekhirev M, Wyatt BC, Anasori B, Gogotsi Y, Seh ZW (2022) Fundamentals of MXene synthesis. Nature Synthesis 1: 601–614. https://doi.org/10.1038/s44160-022-00104-6

Lipatov A, Sinitskii A (2019) Electronic and Mechanical Properties of MXenes Derived from Single-Flake Measurements. In: Anasori B, Gogotsi Y (Eds) 2D Metal Carbides and Nitrides (MXenes): Structure, Properties and Applications. Springer International Publishing, Cham, 301–325. https://doi.org/10.1007/978-3-030-19026-2_16

Liu M, Wang Z, Song P, Yang Z, Wang Q (2021) Flexible MXene/rGO/CuO hybrid aerogels for high performance acetone sensing at room temperature. Sensors and Actuators B: Chemical 340: 129946. https://doi.org/10.1016/J.SNB.2021.129946

Liu Y, Xiao H, Goddard WA (2016) Schottky-Barrier-Free Contacts with Two-Dimensional Semiconductors by Surface-Engineered MXenes. Journal of the American Chemical Society 138: 15853–15856. https://doi.org/10.1021/JACS.6B10834

Ma Z, Jiang R, Zhang Y, Ma L, Bai Y, Zhang K, Zuo X, Zuo Y, Jing H, Qin J, Zhang G (2025) Lightweight and mechanically strong MXene-Based microcellular nanocomposite foams for integrated electromagnetic interference shielding and thermal management. Composites Science and Technology 260: 110988. https://doi.org/10.1016/J.COMPSCITECH.2024.110988

Malaki M, Maleki A, Varma RS (2019) MXenes and ultrasonication. Journal of Materials Chemistry A 7: 10843–10857. https://doi.org/10.1039/c9ta01850f

Mayerberger EA, Urbanek O, McDaniel RM, Street RM, Barsoum MW, Schauer CL (2017) Preparation and characterization of polymer-$Ti_3C_2T_x$ (MXene) composite nanofibers produced via electrospinning. Journal of Applied Polymer Science 134: 45295. https://doi.org/10.1002/APP.45295

Mirzaei A, Kim JY, Kim JH, Nam MS, Kim HW, Kim SS (2024) Accordion-like $Ti_3C_2T_x$ MXene with high flexibility for NH_3 sensing in self-heating mode. Ceramics International 51: 2930–2946. https://doi.org/10.1016/J.CERAMINT.2024.11.270

Mohammadi AV, Rosen J, Gogotsi Y (2021) The world of two-dimensional carbides and nitrides (MXenes). Science 372: eabf1581. https://doi.org/10.1126/science.abf1581

Mohtasim MS, Das BK (2025) MXene based composite phase change materials for thermal energy storage applications: Featuring bio-mimic approaches. Renewable and Sustainable Energy Reviews 207: 114952. https://doi.org/10.1016/J.RSER.2024.114952

Naguib M, Barsoum MW, Gogotsi Y (2021) Ten years of progress in the synthesis and development of MXenes. Advanced Materials 33: 2103393. https://doi.org/10.1002/adma.202103393

Naguib M, Unocic RR, Armstrong BL, Nanda J (2015) Large-scale delamination of multi-layers transition metal carbides and carbonitrides "MXenes." Dalton Transactions 44: 9353–9358. https://doi.org/10.1039/c5dt01247c

Naguib M, Saito T, Lai S, Rager MS, Aytug T, Parans Paranthaman M, Zhao MQ, Gogotsi Y (2016) $Ti_3C_2T_x$ (MXene)–polyacrylamide nanocomposite films. RSC Advances 6: 72069–72073. https://doi.org/10.1039/C6RA10384G

Natu V, Sokol M, Verger L, Barsoum MW (2018) Effect of Edge Charges on Stability and Aggregation of $Ti_3C_2T_z$ MXene Colloidal Suspensions. The Journal of Physical Chemistry C 122: 27745–27753. https://doi.org/10.1021/ACS.JPCC.8B08860

Nguyen TL, Bao Trang NT, Anh Duy NV, Thu Hoa NT, Dang MT (2025) First-principles insights into selenium and sulfur doping on Ti_2CO_2 MXene for mitigating the shuttle effect in lithium–sulfur batteries. Advances in Natural Sciences: Nanoscience and Nanotechnology 16: 045008. https://doi.org/10.1088/2043-6262/AE0B6F

Nie J, Zhang X, Wang M, Ou Y, Li S, Zhong P, Wang W, Zhu G, Ma X (2025) MXene quantum dots decorated g-C_3N_4/BiOI heterojunction photocatalyst for efficient NO deep oxidation and CO_2 reduction. Separation and Purification Technology 354: 128961. https://doi.org/10.1016/J.SEPPUR.2024.128961

Novoselov KS, Geim AK, Morozov S V, Jiang D, Zhang Y, Dubonos S V, Grigorieva I V, Firsov AA (2004) Electric field effect in atomically thin carbon films. Science 306: 666–669. https://doi.org/10.1126/science.1102896

Pranada E, Ngozichukwu B, Yoo R, Johnson D, Barteau MA, Abdel-Wahab A, Djire A (2025) Hydrogen Evolution and Oxygen Reduction on OH/F-Terminated Titanium Nitride MXene Reveal the Role of the Surface Termination Group in Electrocatalysis. ACS Catalysis 15: 982–991. https://doi.org/10.1021/ACSCATAL.4C05247

Qiao C, Wu H, Xu X, Guan Z, Ou-Yang W (2021) Electrical Conductivity Enhancement and Electronic Applications of 2D $Ti_3C_2T_x$ MXene Materials. Advanced Materials Interfaces 8: 2100903. https://doi.org/10.1002/ADMI.202100903

Rafiq S, Awan SU, Zheng RK, Wen Z, Rani M, Akinwande D, Rizwan S (2020) Novel room-temperature ferromagnetism in Gd-doped 2-dimensional $Ti_3C_2T_x$ MXene semiconductor for spintronics. Journal of Magnetism and Magnetic Materials 497: 165954. https://doi.org/10.1016/J.JMMM.2019.165954

Sadashiva S, Chakraborty I, Havanagi SS, Sonali, Mazumder N, Singh BN (2024) Recent developments in MXene-based materials for biomedical applications in regenerative medicine. MXenes: From Research to Emerging Applications: 29–48. https://doi.org/10.1201/9781003366225-3

Samiei S, Iraji zad A, Kalantarian A, Mirsepah A (2026) MoS_2/MXene bilayer quartz crystal microbalance sensor with enhanced sensitivity and selectivity for room-temperature xylene detection. Microchimica Acta 193: 340. https://doi.org/10.1007/S00604-026-07952-5

Scheibe B, Tadyszak K, Jarek M, Michalak N, Kempiński M, Lewandowski M, Peplińska B, Chybczyńska K (2019) Study on the magnetic properties of differently functionalized multilayered $Ti_3C_2T_x$ MXenes and Ti-Al-C carbides. Applied Surface Science 479: 216–224. https://doi.org/10.1016/J.APSUSC.2019.02.055

Sheoran M, Gupta S, Sharma R, Sinha OP (2025) Insights on $MnCo_2O_4$ spinel nanostructures for supercapacitor application: as electrode material. Advances in Natural Sciences: Nanoscience and Nanotechnology 16: 023002. https://doi.org/10.1088/2043-6262/ADB55D

Shuck CE, Gogotsi Y (2020) Taking MXenes from the lab to commercial products. Chemical Engineering Journal 401: 125786. https://doi.org/10.1016/j.cej.2020.125786

Singh S, Dharavath S, Kodali S, Dash RK (2025) The role of delaminating agents on the structure, morphology, bonding, and electrical properties of HF etched MXenes. FlatChem 49: 100806. https://doi.org/10.1016/J.FLATC.2024.100806

Song H, Ma Y, Yao Q, Liu C, Li X, Tao X (2024) Freeze-sonication delamination method of high crystalline-quality MXene with high yield. Chemical Engineering Journal 491: 151909. https://doi.org/10.1016/J.CEJ.2024.151909

Sreedhar A, Noh JS (2025a) Advancements in $Ti_3C_2T_x$ MXene-Integrated Various Metal Hydrides for Hydrogen Energy Storage: A Review. Nanomaterials 15: 673. https://doi.org/10.3390/NANO15090673

Sreedhar A, Noh JS (2025b) Role of emerging 2D Nb_2CT_x MXene for multiple toxic matter degradation, H_2 generation, and H_2 storage applications: A review. Journal of Water Process Engineering 75: 107996. https://doi.org/10.1016/J.JWPE.2025.107996

Sreedhar A, Ta QTH, Noh J-S (2022) Advancements in the photocatalytic activity of various bismuth-based semiconductor/$Ti_3C_2T_x$ MXene interfaces for sustainable environmental management: A review. Journal of Industrial and Engineering Chemistry 115: 26-47. https://doi.org/10.1016/j.jiec.2022.08.013

Sreedhar A, Ta QTH, Noh J-S (2023a) 2D $Ti_3C_2T_x$ MXene interfaced ZnO/WO_3 thin film nanostructures towards improved photoelectrochemical water splitting. Journal of Electroanalytical Chemistry 940: 117509. https://doi.org/10.1016/j.jelechem.2023.117509

Sreedhar A, Pallavolu MR, Noh JS (2023b) Progress in surface and interlayer distance modulated 2D $Ti_3C_2T_x$ MXenes for potential flexible supercapacitors: A review. Applied Materials Today 35: 101942. https://doi.org/10.1016/J.APMT.2023.101942

Sreedhar A, Ravi P, Noh J-S (2024) Advancements in two-dimensional Ti_3C_2 MXene interfaced semiconductors for room temperature NO_2 gas sensing: A review. Journal of Materials Science & Technology 203: 237-254. https://doi.org/10.1016/j.jmst.2024.04.016

Sreedhar A, Pabba DP, Koyyada G, Alodhayb AN, Pandiaraj S, Reddy NR, Joo SW (2025) Green-synthesized metal oxide nanostructures for solar-driven photocatalysis: Advances, challenges, and environmental applications. Journal of Alloys and Compounds 1036: 182080. https://doi.org/10.1016/J.JALLCOM.2025.182080

Srivatsa S, Tokarz W, Przewoźnik J, Strączek T, Grabowski K, Rutkowski P, Uhl T, Kulawik J, Kata D, Madej D, Lis J, Kapusta C (2024) Temperature Evolution of Composition, Thermal, Electrical and Magnetic Properties of $Ti_3C_2T_x$ -MXene. Materials (Basel, Switzerland) 17: 2199. https://doi.org/10.3390/MA17102199

Stock N, Biswas S (2012) Synthesis of metal-organic frameworks (MOFs): Routes to various MOF topologies, morphologies, and composites. Chemical Reviews 112: 933–969. https://doi.org/10.1021/CR200304E

Sun B, Lv H, Liu Z, Wang J, Bai X, Zhang Y, Chen J, Kan K, Shi K (2021) Co_3O_4@PEI/$Ti_3C_2T_x$ MXene nanocomposites for a highly sensitive NO_x gas sensor with a low detection limit. Journal of Materials Chemistry A 9: 6335–6344. https://doi.org/10.1039/D0TA11392A

Sun W, Xie Y, Kent PRC (2018) Double transition metal MXenes with wide band gaps and novel magnetic properties. Nanoscale 10: 11962–11968. https://doi.org/10.1039/C8NR00513C

Swain KK, Pradhan SK, Late DJ (2025) MXene-Based Nanomaterials for Pollution Remediation: A Review. ChemistrySelect 10: e202404885. https://doi.org/10.1002/SLCT.202404885

Ta QTH, Thakur D, Noh J-S (2022a) Enhanced Gas Sensing Performance of ZnO/$Ti_3C_2T_x$ MXene Nanocomposite. Micromachines 13: 1710. https://doi.org/10.3390/mi13101710

Ta QTH, Tri NN, Noh J-S (2022b) Improved NO_2 gas sensing performance of 2D MoS_2/$Ti_3C_2T_x$ MXene nanocomposite. Applied Surface Science 604: 154624. https://doi.org/10.1016/j.apsusc.2022.154624

Ta QTH, Tran NM, Tri NN, Sreedhar A, Noh JS (2021) Highly surface-active Si-doped TiO_2/$Ti_3C_2T_x$ heterostructure for gas sensing and photodegradation of toxic matters. Chemical Engineering Journal 425: 131437. https://doi.org/10.1016/j.cej.2021.131437

Ta QTH, Nhiem LT, Oanh DTY, Hieu NH, Nguyen PKT (2024) Review on progress in synthesis of CdS-based composites and their potential applications. Vietnam Journal of Chemistry 63: 535–545. https://doi.org/10.1002/VJCH.202400155

Tan Y, Xu J, Li Q, Zhang W, Lu C, Song X, Liu L, Chen Y (2024) Sensitivity-Enhanced, Room-Temperature Detection of NH_3 with Alkalized $Ti_3C_2T_x$ MXene. Nanomaterials 14: 680. https://doi.org/10.3390/NANO14080680

Tang H, Wang R, Shi L, Sheremet E, Rodriguez RD, Sun J (2021) Post-processing strategies for improving the electrical and mechanical properties of MXenes. Chemical Engineering Journal 425: 131472. https://doi.org/10.1016/J.CEJ.2021.131472

Thi QV, Tan HL, Tang KY, Xiong Heng JZ, Loh XJ, Ye E, Sohn D, Truong VX (2024) Innovation in hierarchical metal organic framework derivatives toward electromagnetic wave absorption. Composite Structures 345: 118390. https://doi.org/10.1016/J.COMPSTRUCT.2024.118390

Tran NM, Ta QTH, Noh J-S (2021a) Unusual synthesis of safflower-shaped TiO_2/$Ti_3C_2T_x$ heterostructures initiated from two-dimensional Ti3C2 MXene. Applied Surface Science 538: 148023. https://doi.org/10.1016/j.apsusc.2020.148023

Tran NM, Ta QTH, Sreedhar A, Noh J-S (2021b) $Ti_3C_2T_x$ MXene playing as a strong methylene blue adsorbent in wastewater. Applied Surface Science 537: 148006. https://doi.org/10.1016/j.apsusc.2020.148006

Venkateshalu S, Grace AN (2020) MXenes—A new class of 2D layered materials: Synthesis, properties, applications as supercapacitor electrode and beyond. Applied Materials Today 18: 100509. https://doi.org/10.1016/j.apmt.2019.100509

Wyatt BC, Rosenkranz A, Anasori B (2021) 2D MXenes: Tunable Mechanical and Tribological Properties. Advanced Materials 33: 2007973. https://doi.org/10.1002/ADMA.202007973

Xiong S, Wu J, Chen M, Zhang K, Fang K, Wang X, Hua C, Chu J, Zhang R, Gong M (2025) Interfacial Self-Assembly of $Ti_3C_2T_x$ MXene Thin Films and Their Electrochromic Properties. ACS Applied Electronic Materials 7: 5392–5403. https://doi.org/10.1021/ACSAELM.5C00326

Xu B, Gogotsi Y (2020) MXenes: From Discovery to Applications. Advanced Functional Materials 30: 2007011 https://doi.org/10.1002/adfm.202007011

Yang Y, Anayee M, Pattammattel A, Shekhirev M, Wang R, Huang X, Chu YS, Gogotsi Y, May SJ (2024) Enhanced magnetic susceptibility in $Ti_3C_2T_x$ MXene with Co and Ni incorporation. Nanoscale 16: 5760–5767. https://doi.org/10.1039/D3NR05685F

Yang Z, Jiang L, Wang J, Liu F, He J, Liu A, Lv S, You R, Yan X, Sun P (2021) Flexible resistive NO_2 gas sensor of three-dimensional crumpled MXene $Ti_3C_2T_x$/ZnO spheres for room temperature application. Sensors and Actuators B: Chemical 326: 128828. https://doi.org/10.1016/j.snb.2020.128828

Yang Z, Liu A, Wang C, Liu F, He J, Li S, Wang J, You R, Yan X, Sun P, Duan Y, Lu G (2019) Improvement of Gas and Humidity Sensing Properties of Organ-like MXene by Alkaline Treatment. ACS Sensors 4: 1261–1269. https://doi.org/10.1021/ACSSENSORS.9B00127

Yin T, Li Y, Wang R, Al-Hartomy OA, Al-Ghamdi A, Wageh S, Luo X, Tang X, Zhang H (2021) Synthesis of $Ti_3C_2F_x$ MXene with controllable fluorination by electrochemical etching for lithium-ion batteries applications. Ceramics International 47: 28642–28649. https://doi.org/10.1016/J.CERAMINT.2021.07.023

Zha XH, Luo K, Li Q, Huang Q, He J, Wen X, Du S (2015) Role of the surface effect on the structural, electronic and mechanical properties of the carbide MXenes. Europhysics Letters 111: 26007. https://doi.org/10.1209/0295-5075/111/26007

Zhan X, Si C, Zhou J, Sun Z (2020) MXene and MXene-based composites: synthesis, properties and environment-related applications. Nanoscale Horizons 5: 235–258. https://doi.org/10.1039/C9NH00571D

Zhang H, Wang L, Chen Q, Li P, Zhou A, Cao X, Hu Q (2016) Preparation, mechanical and anti-friction performance of MXene/polymer composites. Materials & Design 92: 682–689. https://doi.org/10.1016/J.MATDES.2015.12.084

Zhang H-F, Xuan J-Y, Zhang Q, Sun M-L, Jia F-C, Wang X-M, Yin G-C, Lu S-Y (2022) Strategies and challenges for enhancing performance of MXene-based gas sensors: A review. Rare Metals 41: 3976–3999. https://doi.org/10.1007/s12598-022-02087-x

Zhang K, Di M, Fu L, Deng Y, Du Y, Tang N (2020) Enhancing the magnetism of 2D carbide MXene $Ti_3C_2T_x$ by H_2 annealing. Carbon 157: 90–96. https://doi.org/10.1016/J.CARBON.2019.10.016

Zhang W, Zhang X (2022) The effect of ultrasound on synthesis and energy storage mechanism of $Ti_3C_2T_x$ MXene. Ultrasonics Sonochemistry 89: 106122. https://doi.org/10.1016/J.ULTSONCH.2022.106122

Zhang Z, Ji Y, Jiang Q, Xia C (2024) Molten-salt synthesized MXene for catalytic applications: A review. Chemical Physics Reviews 5: 031311. https://doi.org/10.1063/5.0215613

Zou S, Gao J, Liu L, Lin Z, Fu P, Wang S, Chen Z (2020) Enhanced gas sensing properties at low working temperature of iron molybdate/MXene composite. Journal of Alloys and Compounds 817: 152785. https://doi.org/10.1016/J.JALLCOM.2019.152785

Additional information

Conflict of interest

The authors declare that they have no conflict of interest and no affiliations with or involvement in any organization or entity with any financial interest in the subject matter or materials discussed in this manuscript.

Ethical compliance

No ethical statement was reported.

Artificial Intelligence (AI) use

During preparation of the revised submission, the authors used ChatGPT, provided by OpenAI, to improve grammar and readability of the manuscript. After using this service, the authors reviewed and edited the content as needed and take full responsibility for the content of the publication.

Funding statement

No funding was reported.

Author contributions

Qui Thanh Hoai Ta: Conceptualization, Data curation, Writing – original draft; Pham Ngoc Nhiem: Formal analysis, Writing – original draft; Quynh Nhu Tran: Formal analysis, Writing – original draft; Lu Thi Mong Thy: Formal analysis, Writing – original draft; Jin-Seo Noh: Writing - review and editing, Supervision

Author ORCIDs

Qui Thanh Hoai Ta https://orcid.org/0000-0002-0387-6281

Nhiem Pham-Ngoc https://orcid.org/0009-0005-2869-9495

Quynh Nhu Tran https://orcid.org/0000-0002-3004-0121

Lu Thi Mong Thy https://orcid.org/0009-0009-2233-438X

Jin-Seo Noh https://orcid.org/0000-0002-6700-0238